Multi-Agent Dynamic Ergodic Search with Low-Information Sensors

Howard Coffin[1], Ian Abraham[2], Guillaume Sartoretti[3], Tyler Dillstrom[4], Howie Choset[1]

***Abstract*— The long-term goal of this work is to enable agents with low-information sensors to perform tasks usually restricted to ones with more sophisticated, high-information sensing capabilities. Our approach is to regulate the motion of these low-information agents to obtain "high-information" results. As a first step, we consider a multi-agent system tasked with locating and tracking a moving target using only noisy binary sensors that measure the presence (or lack thereof) of a target in the sensor's field of view. To generate effective paths for these agents, we use ergodic trajectory optimization with a novel mutual information map that is fast to compute and can handle the discontinuous measurement models often associated with low-information sensing. We compare our approach with existing motion planning methods in multiple simulated experiments. Our experiments show that agents using our method outperform purely coverage-based approaches as well as naive ergodic approaches.**

I. Introduction

This work considers the question: can well-designed motion strategies allow agents with low-information sensors to perform complex information-gathering tasks like target search? As their name suggests, low-information sensors, such as tactile sensors, provide little information compared to high-information sensors like RGB-D cameras. Such low-information sensing can result from either low resolution or high uncertainty in the sensor's measurements. In this work, we propose a motion planning method for a multi-agent system tasked with autonomously locating and tracking a single moving target with binary sensors, a type of low-information sensor that only produces a 0 or 1 indicating whether the target is within each agent's field of view (FOV).

In order to plan effective motion strategies for these agents with binary sensors, we use ergodic trajectory optimization (ETO), a framework which has been applied to many information-gathering problems, including target search [1]–[6], self localization and learning [7], [8], shape estimation [9], and robotic palpation [10]. The ETO framework has been shown to produce effective long-term motion strategies for exploration [5]. Since low-information sensors, by their very nature, cannot gather much information in a short time, the ETO framework's utility for long-term motion strategies makes it appealing for systems with low-information sensors.

[1]H. Coffin and H. Choset are with the Robotics Institute at Carnegie Mellon University, Pittsburgh, PA 15213, USA. howard2706@gmail.com, choset@andrew.cmu.edu

[2] I. Abraham is with the Department of Mechanical Engineering at Yale University, New Haven, CT 06511 USA. ian.abraham@yale.edu

[3] G. Sartoretti is with the Department of Mechanical Engineering at the National University of Singapore, 117575 Singapore. mpegas@nus.edu.sg

[4] T. Dillstrom is with Northrop Grumman Corporation at Falls Church, VA. vernon.dillstrom@ngc.com

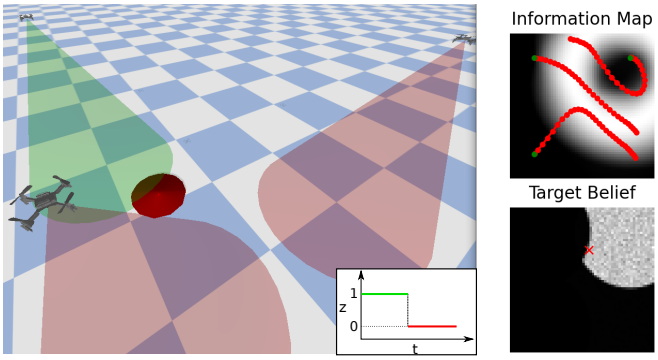

Fig. 1. **Illustration of multi-agent search with binary detection sensor.** (Left) Snapshot of the simulation environment. Each drone can see the moving red target when it is within the drone's FOV, shown as a cones which turns green when the target is observed and red otherwise. (Right) Example mutual information map and target belief distribution (lighter is higher). Green dots are current drone (x, y) positions and red dots show planned ergodic trajectories over a time horizon $t_H = 30$. Red $\times$ shows true target (x, y) location (unknown to agents).

In ETO, agents' trajectories are optimized so that the time spent in a region of the search space is proportional to the amount of information in that area, according to an *a priori* information map [11]. Though previous works have primarily used heuristic-based maps [1], [4], [10], [11] or Fisher information maps [2], [3], [7], [9], we propose to use a mutual information map. Mutual information, unlike Fisher information, can handle measurement models which are discontinuous with respect to sensor location [12]. Previous methods for computing a mutual information map have relied on learning-based techniques which require large amounts of data to train and can be computationally burdensome [13]. We instead derive a quick-to-compute, closed-form expression for the mutual information for the specific case of a low-information binary target sensor.

We use this ETO-based method for motion planning to search for a moving target using only binary target sensors and demonstrate that our proposed mutual information map allows the agents to effectively locate and track the target. We compare our method to existing techniques on a number of simulated examples with a multi-agent system and show that ours results in the best estimate of the target's location (in terms of mean absolute distance).

A summary of contributions in this work is as follows:

1) Extending existing ergodic search techniques for use with low-information binary target sensors.
2) Deriving a quick-to-compute closed-form expression for the mutual information between binary observations and a target belief distribution.

II. Related Works

A. Low-Information Sensors

Often, simpler, low tech sensors can be cheaper or more reliable than sensors which provide higher quality information. For example, while a high-resolution camera could provide lots of information about a persons location in its field of view, it might cost more than the rest of the robot and still fail when lighting is poor. A pyro-electric infrared sensor is both cheap and requires no lighting at all to detect a person, though the information gained from a detection is significantly lower.

For these reasons, low-information sensors have widely been used in various robotics-related domains. Acoustic binary proximity sensors, pyro-electric infrared sensors, and moving target indicators are often used in static wireless sensor networks to track moving objects in a fixed region which are used in applications such as disaster relief and surveillance [14]–[20]. Gas sensors have been used on teleoperated mobile robots to locate hazardous gas leaks [20], and tactile sensors have been used for SLAM with fixed agent trajectories [21], [22]. In contrast to these works, which are concerned with statically placed sensors or human controlled agents, we focus on autonomous agents, more in line with works like [9]. The work in [9] considers the active non-parametric shape estimation problem with a tactile sensor, but relies on a learned collision likelihood distribution to smooth out discontinuities resulting from the sensor only measuring contact or no contact. In this work, we present a method that is indifferent to discontinuities, allowing us to use an exact measurement model and avoid the parameter tuning required in most learning-based approaches.

B. Information Theoretic Planning

Information theoretic planning has been considered for many different information gathering problems and has been particularly successful at addressing the target search problem, where agents are tasked with locating and tracking a moving target. With these methods, agents are controlled so that sensor measurements they take are likely to reduce uncertainty about the target location [23]. In [15], the authors use a particle filter based estimate of α-mutual information (Rényi information) for static but configurable binary sensors to create short time horizon plans for target tracking. Other works consider information maximizing control methods for mobile agents using various types of sensors [23], [24]. However, these works run into a fundamental problem with information-maximizing strategies; the computation time for both mutual information and Rényi information scale exponentially with the number of agents and the time horizon for planning. Due to computational constraints, these early works choose actions over a maximum time horizon of two, leading to myopic behavior that can result in failure to locate targets.

Recent works have developed less greedy methods using combination of computationally cheaper approximations of the information gain and more efficient planning methods. In [25], the authors derive an approximate form for the mutual information when the measurement model is Gaussian, and alleviate some of the issues of greedy planning by carefully choosing the set of motion primitives to avoid considering primitives which collect similar information. Other works consider sample-based planning techniques for information acquisition over long time horizons [26], [27]. Dames [28] considers many ways to make computing the mutual information more computationally feasible—for example, the use of an adaptive cellular representation for the target belief distribution. However, these works do not get over the fundamental scaling issues of information maximization.

C. Ergodic Search

Ergodic search is another technique that has been applied to the target search problem. In the ETO framework, trajectories are optimized so that the agents visit areas of the search space with a frequency proportional to the amount of information in that area, according to a static information map [11]. This search strategy allows for the planning of long-time horizon trajectories which balance between exploitation of areas of high information and exploration of low-information regions, even when the distribution of information is highly non-convex [5]. Because the information map is static (at least over the course of one planning step), it does not fully consider how every measurement interacts with the others like purely information-based approaches. However, computation of the ergodic metric scales linearly instead of exponentially like most information metrics, allowing it to be used with more agents and longer planning horizons.

In [1] and [4], the authors use this framework for target search with a heuristic-based map defined by the target belief distribution. In this work, we show that using the target belief distribution as the information map is not always effective for binary sensors as just maximizing the likelihood of observing the target may not be enough to get a good estimate of its location. Both [3] and [2] consider sensors with non-linear measurement models and use ETO with a information map defined using the Fisher information matrix determinant in order to get more informative measurements. Though maximizing the Fisher information is desirable, as it can be used to derive a lower bound for the variance of an unbiased estimator for a target location [12], it requires the measurement model to be differentiable. Otherwise, the Fisher Information does not exist at every point. For the binary sensors considered in this paper, using Fisher information is particularly impractical as it is always either zero or undefined.

III. Problem Setup

In this section, we describe the method used to actively search for and localize a moving target. We first define the target dynamics and the measurement model of the binary sensors used to track the target. Then, we describe the model predictive control procedure we use to optimize the ergodic metric, the cost function associated with ETO.

A. Target Tracking

Let $y_t \in \mathcal{Y}$ be the target's state at time t, where $\mathcal{Y}$ is the set of all possible target states; in this paper, where we are tracking a single target in the plane, $\mathcal{Y} \subset \mathbb{R}^2$. Note that if the target is a point mass, then y_t is simply the location of that point, and if the target is a disk (as in Figure 1), y_t is some reference point on the disk, e.g., its center. Furthermore, let $g(y_{t+1}|y_t)$ be the probability density function representing the non-adversarial, stochastic dynamics of the target.

In order to locate the target, each agent (enumerated as $i \in \{1, \dots, N\}$) has a binary sensor which outputs stochastic measurements $z_{i,t} \in \{0, 1\}$ indicating the presence of the target in the sensor's FOV. The state of agent i at time t is $x_{i,t} \in \mathcal{X}$, where $\mathcal{X}$ is the set of achievable agent states, and we call $S(x_{i,t}) \subseteq \mathcal{Y}$ the agent's sensor footprint, which gives the set of target locations within the sensor's FOV when the agent is at $x_{i,t}$. We also define $T, F \in [0, 1]$ as the true and false positive rates of the binary sensors, giving us the following measurement model:

$$z_{i,t} \sim \begin{cases} \text{Bernoulli}(T) & \text{if } y_t \in S(x_{i,t}) \\ \text{Bernoulli}(F) & \text{if } y_t \notin S(x_{i,t}). \end{cases} \tag{1}$$

Let $h(z_{i,t}|y_t; x_{i,t})$ be the probability mass function associated with the distribution for $z_{i,t}$. Note that $h(z_{i,t}|y_t; x_{i,t})$ is conditioned on y_t since this value is unknown to the agents, but parameterized by $x_{i,t}$, which is known.

During target search, we keep track of a target belief distribution with density $b(y_t|z_{0:t}; x_{0:t})$, where $z_{0:t} = [z_{0,0}, \cdots, z_{N,t}]$ is a vector of all the past observations and similarly $x_{0:t} = [x_{0,0}, \cdots, x_{N,t}]$ is a vector of all past agent positions, using the standard recursive Bayes filtering equations (see [29] for details).

B. Ergodic Trajectory Optimization

In ETO, the spatial statistics of agents' trajectories are optimized to cover $\mathcal{X}$ proportional to an *a priori* information map $\Phi : \mathcal{X} \to \mathbb{R}^+$ [11]. We assume that the state of the agent evolves according to the discrete time dynamics

$$x_{i,t+1} = f(x_{i,t}, u_{i,t}), \tag{2}$$

where $u_{i,t} \in \mathcal{U}$ is the control input for agent i at time t. The spatial statistics of the agents' joint trajectory over a time horizon t_H, $\mathbf{x} = [x_{0,t}, \cdots, x_{N,t+t_H-1}]$, are defined as

$$C(x) = \frac{1}{N t_H} \sum_{i=1}^{N} \sum_{\tau=t}^{t+t_H-1} \delta(x - x_{i,\tau}), \tag{3}$$

where δ is the Dirac-delta function. In [11], the authors define the ergodic metric $\mathcal{E}(\mathbf{x})$, which compares the spatial statistics C with the information map Φ, i.e.,

$$\mathcal{E}(\mathbf{x}) = \sum_{k \in \mathbb{Z}^{*n}} \Lambda_k |c_k - \phi_k|^2, \tag{4}$$

where c_k and ϕ_k are the kth Fourier components of C and Φ respectively, and Λ_k are weights which put emphasis on lower-order fourier coefficients [11]. Similarly to [7], we optimize the joint controls $\mathbf{u} = [u_{0,t}, \cdots, u_{N,t+t_H-1}]$ in a receding horizon fashion with the optimization

$$\begin{gathered} \mathbf{u}^\star = \arg\min_{\mathbf{u}} \mathcal{E}(\mathbf{x}) + \sum_i \sum_t u_{i,t}^\top R u_{i,t} \\ \text{subject to } x_{i,t+1} = f(x_{i,t}, u_{i,t}) \text{ and } l(\mathbf{x}, \mathbf{u}) \leq 0 \\ \text{with initial condition } x_{0,0}, \dots, x_{N,0}, \end{gathered} \tag{5}$$

where R is a matrix that penalizes control effort and l is a set of inequality constraints on the trajectory and controls e.g., inter-agent distance and control saturation.

There exists many different methods for performing this optimization [3], [7], [30]. We solve Equation 5 using the automatic differentiation library CasADi [31]. An example trajectory with $t_H = 30$ is shown in Figure 1.

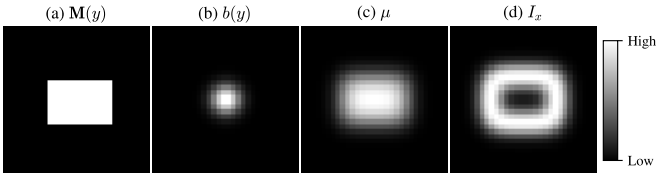

Fig. 2. **Components for calculating the mutual information map.** (a) Sensor footprint mask $\mathbf{M}(y)$ for a rectangular sensor footprint, (b) Current belief about target location $b(y)$, (c) $\mu(x)$ calculated using Equation 16 (shown projected onto $\mathcal{Y}$), (d) $I_x(y; z)$ calculated using Equation 9 (shown projected onto $\mathcal{Y}$)

IV. Information Map with Binary Target Sensors

Now, we derive an information map for a binary target sensor to use with ETO. We first give some background on mutual information. Then, we show how a closed form expression for both metrics can be derived and used to compute corresponding information maps.

A. Mutual Information

Mutual information is a commonly used measure for information in the target search problem [24]–[26], [28]. The mutual information between an observation z and the target belief for y when an agent is at state x is

$$\begin{aligned} I_x(y; z) &= \mathbb{E}_{h(z;x)}[D_{KL}(b(y|z; x) \;||\; b(y))] \\ &= D_{KL}(p(y, z; x) \;||\; b(y)h(z; x)) \\ &= H(y) - H(y|z; x), \end{aligned} \tag{6}$$

where $\mathbb{E}$ is the expected value, D_{KL} is the Kullback-Leibler (KL) divergence, and H is the Shannon entropy [12]. It can be viewed both as a measure for how dependent the target location y and an observation z are (line 2 of Equation 6) and as the expected reduction in uncertainty in y from making an observation z (line 3 of Equation 6). We can simply normalize $I_x(y; z)$ over $\mathcal{X}$ to create an information map to use with ETO,

$$\Phi(x) = \frac{I_x(y; z)}{\int_{\mathcal{X}} I_{x'}(y; z) dx'} \tag{7}$$

B. Derivations and Computation for a Binary Sensor

In this subsection, we discuss the computation of information maps based on the mutual information which can be used with ETO to produce effective search trajectories. We

first define $\mu(x)$ to be the measure of the set $S(x)$ (the sensor footprint) over the target belief distribution, i.e.,

$$\mu(x) = \int_{S(x)} b(y)dy. \tag{8}$$

Proposition 1: For the binary measurement model described in Equation 1, the mutual information (Equation 6) between a sensor observation z and the target belief distribution for y when an agent is in state x is

$$\begin{aligned} &I_x(y;z) = \\ &\mu(x)\left(T\log\left(\frac{T}{p_1}\right) + (1-T)\log\left(\frac{1-T}{p_0}\right)\right) + \\ &(1-\mu(x))\left(F\log\left(\frac{F}{p_1}\right) + (1-F)\log\left(\frac{1-F}{p_0}\right)\right), \end{aligned} \tag{9}$$

where $p_1 = T\mu(x) + F(1-\mu(x))$ and $p_0 = 1 - p_1$ are the believed probabilities of observing a 1 and 0 respectively.

Proof: We start with the definition of mutual information using KL divergence in Equation 6 and rewrite it to use the conditional distribution of z on y.

$$\begin{aligned} I_x(y;z) &= D_{KL}(b(y,z;x) \;||\; b(y)h(z;x)) \\ &= \int_{\mathcal{Y}} \sum_{z\in\{0,1\}} p(y,z;x)\log\left(\frac{p(y,z;x)}{b(y)h(z;x)}\right)dx \\ &= \int_{\mathcal{Y}} \sum_{z\in\{0,1\}} h(z|y;x)b(y)\log\left(\frac{h(z|y;x)}{h(z;x)}\right)dx. \end{aligned} \tag{10}$$

Then, we can write $h(z;x)$ in terms of $\mu(x)$, T, and F using Equation 1 and the law of total probability.

$$\begin{aligned} h(z=1;x) &= \int_{\mathcal{Y}} h(z=1|y;x)b(y)dy \\ &= T\int_{S(x)} b(y)dy + F\int_{S^c(x)} b(y)dy \\ &= T\mu(x) + F(1-\mu(x)) := p_1 \end{aligned} \tag{11}$$

$$\begin{aligned} h(z=0;x) &= 1 - h(z=1;x) \\ &= 1 - T\mu(x) - F(1-\mu(x)) := p_0 \end{aligned} \tag{12}$$

where p_1 and p_0 are defined for notational convenience and $S^c(x)$ is the set complement of $S(x)$. Then, by splitting up the integral over $\mathcal{Y}$ in Equation 10 by $S(x)$, we get

$$\begin{aligned} &I_x(y;z) = \\ &\int_{S(x)} b(y)\left[T\log\left(\frac{T}{p_1}\right) + (1-T)\log\left(\frac{1-T}{p_0}\right)\right]dy + \\ &\int_{S^c(x)} b(y)\left[F\log\left(\frac{F}{p_1}\right) + (1-F)\log\left(\frac{1-F}{p_0}\right)\right]dy. \end{aligned} \tag{13}$$

Since all the variables in the square brackets are constant with respect to y, we can substitute in the definition for $\mu(x)$ to get the final expression in Equation 9. ■

Writing $I_x(y,z)$ in terms of $\mu(x)$ is important because, when $S(x)$ is a fixed shape (i.e., it doesn't rotate or scale) which translates around the search space, $\mu(x)$ can be efficiently computed using image convolution. To give a mathematical definition for a fixed shape, we start by defining the projection function $\mathcal{P}(x) : \mathcal{X} \to \mathcal{Y}$, which maps x to its projection on $\mathcal{Y}$ (e.g., if $y = (y_1, y_2)$ and $x = (y_1, y_2, \dot{y}_1, \dot{y}_2, x_5, x_6)$ then $\mathcal{P}(x) = (y_1, y_2)$). Then, $S(x) = S_{\mathcal{P}}(\mathcal{P}(x))$ is a fixed shape iff for all x, y_1, y_2

$$y_1 \in S_{\mathcal{P}}(\mathcal{P}(x)) \iff y_1 + y_2 \in S_{\mathcal{P}}(\mathcal{P}(x) + y_2). \tag{14}$$

This definition captures the idea that $S(x)$ only translates with $\mathcal{P}(x)$ and allows us derive a formula for $\mu(x)$. From $S_{\mathcal{P}}$, we define the mask

$$\mathbf{M}(y) := \mathbf{1}[y \in S_{\mathcal{P}}(\mathbf{0})], \tag{15}$$

where $\mathbf{1}[\cdot]$ is the indicator function. This allows us to calculate $\mu(x)$ as

$$\begin{aligned} \mu(x) &= \int_{S(x)} b(y)dy = \int_{\mathcal{Y}} \mathbf{M}(y - \mathcal{P}(x))b(y)dy \\ &= (\mathbf{M} * b)(\mathcal{P}(x)), \end{aligned} \tag{16}$$

where $*$ is the convolution operator. Using a grid based representation of the target belief distribution and the sensor footprint mask, we can use image convolution to efficiently calculate $\mu(x)$ for all values of x on the grid. Figure 2 shows an example where the sensor footprint is a rectangle. Once we have $\mu(x)$, we can calculate $I_x(y;z)$ using Equation 9.

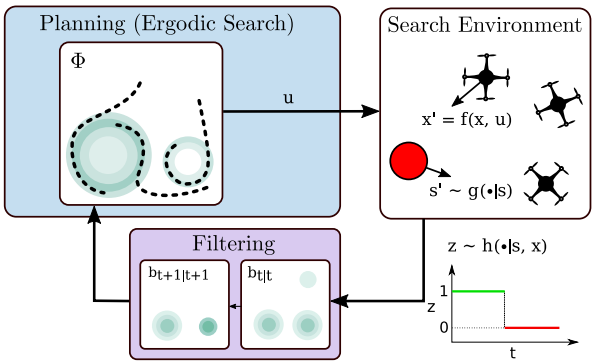

Fig. 3. **ETO pipeline for target search.** The ergodic search algorithm is initialized with a uniform information map Φ which is used to provide an initial exploratory control signal to the agents subject to the optimization described in (5). Subsequent binary sensor measurements acquired through exploration are used to filter the belief over the targets which is used to reconstruct Φ according to Eq. 9.

V. Results

In this section, we compare the performance of our method to a naive ETO implementation and to Boustrophedon decomposition [32] (i.e., "lawnmower" coverage). Additionally, we examine how our method fares as the number of searching agents varies and show that the information map used with ETO can have even more effect on the search performance than the quality of the sensor data received.

A. Experimental Setup

Figure 3 illustrates the pipeline used for the ETO based algorithms. The information map Φ is initially generated as a uniform distribution over the space. At each timestep, each agent moves according the commanded controls based on the initial information map. As the agents move about, they take a binary observation, which are used to update

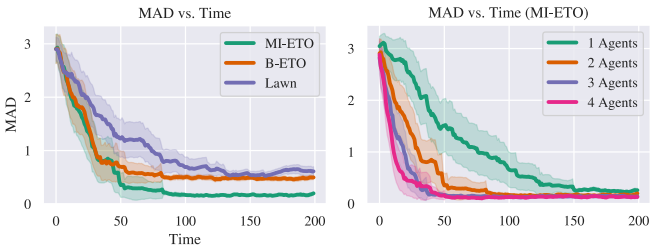

Fig. 4. **Search comparisons and multi-agent contributions.** (Left) Average MAD of the three algorithms $\pm$ two standard errors. Our method (**MI-ETO**) quickly localizes the targets and hones in on their location, as can be seen by the sharp decrease in MAD and low steady state MAD once the targets have been found. (Right) Average MAD of the **MI-ETO** algorithm $\pm$ 2 standard errors with varying numbers of agents. As can be expected, more agents results in better localization but the increase is diminishing; the difference between 1 and 2 agents is much greater than 2 to 3.

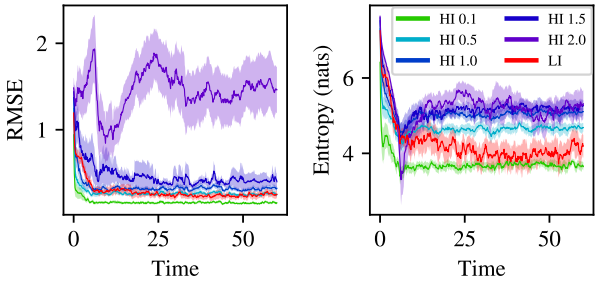

Fig. 5. **Comparison with high information sensors.** (Left) RMSE $\pm$ 2 SE for both higher-information sensors with **B-ETO** (HI) and low-information sensor with **MI-ETO** (LI). The number next to HI is the value of σ^2. (Right) Entropies $\pm$ 2 SE for high and low information sensors. Using **MI-ETO** with a low-information sensors starts to outperform **B-ETO** with the higher-information sensors at around $\sigma^2 = .5$.

the belief about the target's location using a particle filter. Finally, the new belief is used to update the information map Φ according to Eq. 9 which is then inputted into ETO to plan agent trajectories and output corresponding controls. In Boustrophedon decomposition, the trajectories of the agents are fixed to the lawnmower patterns so no replanning is necessary.

To compare performance, we use mean absolute distance (MAD). For a belief b, MAD is defined as

$$\int_{\mathcal{Y}} b(y_t)\ ||y_t - y_t^*||_2\ dy, \tag{17}$$

where y_t^* is the true location of the target and $||y_t - y_t^*||_2$ is the euclidean distance between the state y_t and the true state y_t^*. For the particle filter implementation of the belief used in this work, this is calculated as

$$\sum_i w_i\ ||y_i - y_t^*||_2, \tag{18}$$

where y_i is particle i's state and w_i its corresponding weight. MAD is low when the belief is dense near the true target state (i.e., all the particles are near the true state).

For all the experiments done, the true positive rate T and false positive rate F are set to 0.8 and 0.01 respectively. The search space is a 6 by 6 meter area, and the belief is initialized to a uniform distribution over the space. The agents can move up to 5 m/s and the targets move according to a random walk with a maximum velocity of 0.15 m/s. The field of view of each of the agents is a circular area centered directly below them with radius 0.577 m.

B. Comparisons between Algorithms

The three algorithms compared are as follows: **1. MI-ETO**: ETO with our mutual information-based information map generated using Equation 7; **2. B-ETO**: Naive implementation of ETO, where the the information map is simply the belief $b(y_{t+1}|z_{0:t}; x_{0:t})$ (i.e., not using any information-like measure and simply exploring high likelihood areas); **3. Lawn**: Agents move back and forth across the search space, covering the whole space but not spending additional time in any one area.

Figure 4 shows the average MAD from 40 simulated trials of each algorithm. As can be seen, the **Lawn** algorithm performs the worst as it is not able to take advantage of previously obtained observations. Additionally, the agents do not revisit areas previously covered, meaning that even when the target is detected it is not necessarily tracked afterwards. The **B-ETO** algorithm performs slightly better but still has a high steady-state MAD as the agents are not using an information-based search strategy. Without using mutual information, the agents' sensor observations are not as useful as the **MI-ETO** algorithm. The reason for the disparity between the two ETO algorithms is the binary sensing modality. As can be seen in Figure 2, the information gained by the binary sensors is actually quite low when the agents is directly over an area of high belief, and instead is maximized when $\mu(x)$ is about 0.5. In fact, without providing a full proof due to space constraints, it can be shown that Equation 9 is maximized when $\mu(x)$ is between .5 and $1/e$ (Euler's number) depending on the values of the true and false positive rates T and F. This means that the **B-ETO** is often sending agents to locations with too high a density and therefore doesn't gain as much information.

C. Varying the Number of Agents

Now, we look at how **MI-ETO** performance changes as the number of searching agents varies. The data is collected over 40 simulated trials with each number of searching agents. Illustrated in Figure 4, **MI-ETO** performs significantly worse with one and two agents and that the increased performance diminishes as the number of agents increases (e.g., the difference between 1 and 2 agents is much greater than between 3 and 4). This is an expected result since, as the number of agents increases, the agents' field of views will inevitably overlap during the search process and therefore the information gained by each individual agent will decrease thus reducing efficacy of each contributing agent.

D. Comparison to a High Information Sensor

Here, we show that planning can have a greater effect on the search performance than sensor quality alone. We compare **MI-ETO** to **B-ETO** with varying levels of sensor quality (i.e., noise levels). While the agents using **MI-ETO** still receive only binary observations, the **B-ETO** agents additionally observe $\hat{y} \sim \varphi$. For a true detection, φ represents an estimated location of the target (e.g., from a lidar detector) and is defined by a multivariate normal distribution with

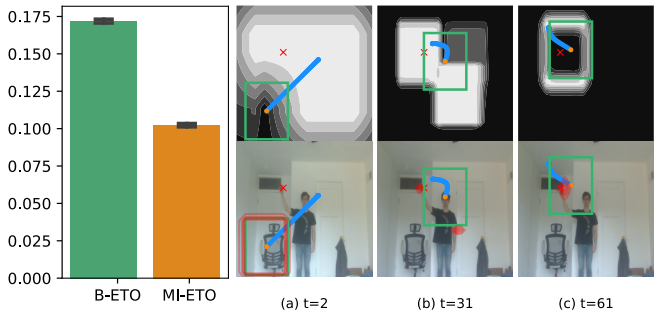

Fig. 6. **Camera-based search and persistent tracking.** (Left) Average RMSE from 10 runs using camera based object detection system from $t = 300$ to $t = 1500$ (steady state tracking). **MI-ETO** performs significantly better than **B-ETO**. (Right) Snapshots of a "robot" with a rectangular sensor footprint localizing a moving target. The top image in each pair shows the information map (lighter is higher). The bottom images show a contour plot of the target belief distribution (red lines) at each time step on top of the full image from the camera. Both images show the current agent location (orange dot), the current planned trajectory (blue), the sensor footprint (outline shown as green rectangle), and the true target position (red $\times$).

mean $y_{i,t}$ (the true location of the target) and σ^2 variance in each independent direction (i.e., a diagonal covariance matrix). For a false positive detection, φ is a uniform distribution over the agent's FOV. If the two algorithms were equal, the agents using **B-ETO** would have a significant advantage due to the additional information provided by their sensors.

In Figure 5, we vary σ^2 and show that at around $\sigma^2 = .5$ **MI-ETO** starts to outperform **B-ETO** in terms of both root-mean-sqaured-error (RMSE) and entropy despite using lower-information sensors (30 trials of each σ^2 value are done). Note that RMSE is calculated similar to MAD given by

$$\sqrt{\int_{\mathcal{Y}} b(y_t)\ ||y_t - y_t^*||_2^2\ dy}. \tag{19}$$

The difference between the compared algorithms is even more apparent when we look at the entropy of the belief distribution. This data demonstrates that effective search planning can be as or even more important than the quality of the sensor data being received.

E. Results with a Camera-Based Object Detection System

In this subsection, we show results using a webcam-based object detector to demonstrate that **MI-ETO** still outperform the naive **B-ETO** when some of the assumptions are broken; neither the stochastic dynamics of the target $g(y_{t+1}|y_t)$ nor the sensor's measurement model (parameterized by T and F) are known.

The target is a red object which is moved around by a person, and the image classifier predicts either a 0 or a 1 depending on whether there is a sufficiently red object within the cutout (see Fig. 6). On 20 training images collected prior to the trials, the classifier had a 99.5% true positive rate and a 0.7% false positive rate, so we use $T = .995$ and $F = .007$. To mimic a real robot moving around with a camera, we allow the classifier to see and move a rectangular cutout from the full webcam image. Figure 6 shows three timesteps from a single trial. The search space and state space are both the $[0, 1] \times [0, 1]$, where (0, 0) is the bottom left of the full image and (1, 1) is the top right. The initial belief is set to the uniform distribution, and the target's dynamics are assumed to be a zero mean Gaussian which is uncorrelated over time.

Though the values of T and F are overly optimistic due to the relatively small training set and the assumed motion model is not realistic for a person trying to move an object around randomly, we still see notable improvement in tracking performance by using the information based map as can be seen in RMSE plot in Figure 6. This is a direct result of MI-ETO better leveraging search over a more appropriate information map for the low-information sensor.

VI. Conclusion

In this paper, we illustrate that low-information sensors can be used to perform complex information gathering tasks by using effective planning techniques. This is demonstrated in the results, which show that using mutual information for the information map for low-information (binary) sensors results in improved search performance compared to existing approaches. In addition, we show that effective planning and search-based methods provided by ergodic trajectory optimization and intelligently constructed information maps enables low-information sensors to perform comparably to high-information sensors. In future works, we would like to explore generalizing this method for use with a heterogeneous swarm of agents and consider other low-information sensing modalities.

References

[1] G. Mathew, A. Surana, and I. Mezić, "Uniform coverage control of mobile sensor networks for dynamic target detection," in *49th IEEE Conference on Decision and Control (CDC)*, 2010, pp. 7292–7299.

[2] A. Mavrommati, E. Tzorakoleftherakis, I. Abraham, and T. D. Murphey, "Real-time area coverage and target localization using receding-horizon ergodic exploration," *IEEE Transactions on Robotics*, vol. 34, no. 1, pp. 62–80, 2017.

[3] L. M. Miller and T. D. Murphey, "Optimal planning for target localization and coverage using range sensing," in *2015 IEEE International Conference on Automation Science and Engineering (CASE)*. IEEE, 2015, pp. 501–508.

[4] E. Ayvali, H. Salman, and H. Choset, "Ergodic coverage in constrained environments using stochastic trajectory optimization," in *2017 IEEE/RSJ International Conference on Intelligent Robots and Systems (IROS)*. IEEE, 2017, pp. 5204–5210.

[5] L. M. Miller, Y. Silverman, M. A. MacIver, and T. D. Murphey, "Ergodic exploration of distributed information," *IEEE Transactions on Robotics*, vol. 32, no. 1, p. 36–52, Feb 2016.

[6] A. Prabhakar, I. Abraham, A. Taylor, M. Schlafly, K. Popovic, G. Diniz, B. Teich, B. Simidchieva, S. Clark, and T. Murphey, "Ergodic specifications for flexible swarm control: From user commands to persistent adaptation," *Robotics: Science and Systems*, 2020.

[7] I. Abraham, A. Mavrommati, and T. Murphey, "Data-driven measurement models for active localization in sparse environments," in *Proceedings of Robotics: Science and Systems*, Pittsburgh, Pennsylvania, June 2018.

[8] I. Abraham, A. Prabhakar, and T. D. Murphey, "An ergodic measure for active learning from equilibrium," *IEEE Transactions on Automation Science and Engineering*, 2021.

[9] I. Abraham, A. Prabhakar, M. J. Z. Hartmann, and T. D. Murphey, "Ergodic exploration using binary sensing for nonparametric shape estimation," *IEEE Robotics and Automation Letters*, vol. 2, no. 2, pp. 827–834, 2017.

[10] E. Ayvali, A. Ansari, L. Wang, N. Simaan, and H. Choset, "Utility-guided palpation for locating tissue abnormalities," *IEEE Robotics and Automation Letters*, vol. 2, no. 2, pp. 864–871, 2017.

[11] G. Mathew and I. Mezić, "Metrics for ergodicity and design of ergodic

dynamics for multi-agent systems," *Physica D: Nonlinear Phenomena*, vol. 240, no. 4-5, p. 432–442, 2011.

[12] T. M. Cover and J. A. Thomas, *Elements of information theory*, 2nd ed. Wiley-Interscience, 2006.

[13] L. Dressel and M. J. Kochenderfer, "Using neural networks to generate information maps for mobile sensors," in *2018 IEEE Conference on Decision and Control (CDC)*. IEEE, 2018, pp. 2555–2560.

[14] W. Kim, K. Mechitov, J.-Y. Choi, and S. Ham, "On target tracking with binary proximity sensors," in *IPSN 2005. Fourth International Symposium on Information Processing in Sensor Networks, 2005.* IEEE, 2005, pp. 301–308.

[15] C. Kreucher, K. Kastella, and A. O. H. Iii, "Sensor management using an active sensing approach," *Signal Processing*, vol. 85, no. 3, p. 607–624, 2005.

[16] N. Shrivastava, R. Mudumbai, U. Madhow, and S. Suri, "Target tracking with binary proximity sensors," *ACM Transactions on Sensor Networks (TOSN)*, vol. 5, no. 4, pp. 1–33, 2009.

[17] J. Singh, U. Madhow, R. Kumar, S. Suri, and R. Cagley, "Tracking multiple targets using binary proximity sensors," in *Proceedings of the 6th international conference on Information processing in sensor networks*, 2007, pp. 529–538.

[18] G. Tuna, V. C. Gungor, and K. Gulez, "An autonomous wireless sensor network deployment system using mobile robots for human existence detection in case of disasters," *Ad Hoc Networks*, vol. 13, pp. 54–68, 2014.

[19] A. H. Henni, R. B. Bachouch, O. Bennis, and N. Ramdani, "Enhanced multiplex binary pir localization using the transferable belief model," *IEEE Sensors Journal*, vol. 19, no. 18, pp. 8146–8159, 2019.

[20] T. Das, D. J. Sut, V. Gupta, L. Gohain, P. Kakoty, and N. M. Kakoty, "A mobile robot for hazardous gas sensing," in *2020 International Conference on Computational Performance Evaluation (ComPE)*. IEEE, 2020, pp. 062–066.

[21] M. Salman and M. J. Pearson, "Advancing whisker based navigation through the implementation of bio-inspired whisking strategies," in *2016 IEEE International Conference on Robotics and Biomimetics (ROBIO)*. IEEE, 2016, pp. 767–773.

[22] O. Struckmeier, K. Tiwari, M. Salman, M. J. Pearson, and V. Kyrki, "Vita-slam: A bio-inspired visuo-tactile slam for navigation while interacting with aliased environments," in *2019 IEEE International Conference on Cyborg and Bionic Systems (CBS)*, 2019, pp. 97–103.

[23] B. Ristic and B.-N. Vo, "Sensor control for multi-object state-space estimation using random finite sets," *Automatica*, vol. 46, no. 11, pp. 1812–1818, 2010.

[24] B. Grocholsky, J. Keller, V. Kumar, and G. Pappas, "Cooperative air and ground surveillance," *IEEE Robotics & Automation Magazine*, vol. 13, no. 3, pp. 16–25, 2006.

[25] B. Charrow, V. Kumar, and N. Michael, "Approximate representations for multi-robot control policies that maximize mutual information," *Robotics: Science and Systems IX*, 2013.

[26] G. A. Hollinger and G. S. Sukhatme, "Sampling-based robotic information gathering algorithms," *The International Journal of Robotics Research*, vol. 33, no. 9, pp. 1271–1287, 2014.

[27] Y. Kantaros, B. Schlotfeldt, N. Atanasov, and G. J. Pappas, "Asymptotically optimal planning for non-myopic multi-robot information gathering." in *Robotics: Science and Systems*, 2019.

[28] P. Dames, "Multi-robot active information gathering using random finite sets," 2015.

[29] Z. Chen *et al.*, "Bayesian filtering: From kalman filters to particle filters, and beyond," *Statistics*, vol. 182, no. 1, pp. 1–69, 2003.

[30] I. Abraham and T. D. Murphey, "Decentralized ergodic control: distribution-driven sensing and exploration for multiagent systems," *IEEE Robotics and Automation Letters*, vol. 3, no. 4, pp. 2987–2994, 2018.

[31] J. A. E. Andersson, J. Gillis, G. Horn, J. B. Rawlings, and M. Diehl, "CasADi – A software framework for nonlinear optimization and optimal control," *Mathematical Programming Computation*, vol. 11, no. 1, pp. 1–36, 2019.

[32] H. Choset, "Coverage of known spaces: The boustrophedon cellular decomposition," *Autonomous Robots*, vol. 9, no. 3, pp. 247–253, 2000.